



TITLE:

# Volcanic Rocks in the Samburu Hills, Northern Kenya

AUTHOR(S):

KOYAGUCHI, Takehiro

---

CITATION:

KOYAGUCHI, Takehiro. Volcanic Rocks in the Samburu Hills, Northern Kenya. African study monographs. Supplementary issue 1984, 2: 147-179

ISSUE DATE:

1984-03

URL:

<https://doi.org/10.14989/68310>

RIGHT:

## VOLCANIC ROCKS IN THE SAMBURU HILLS, NORTHERN KENYA

Takehiro KOYAGUCHI

*Faculty of Science, University of Tokyo*

**ABSTRACT** Volcanic rocks of the Samburu Hills are composed mainly of basaltic lava flows (ankaramite, olivine basalt and hawaiite) intercalated with differentiated rock lava flows and welded tuffs (trachyte and alkali rhyolite).

Basaltic rocks of various ages, from Miocene to Recent, were collected from an area of  $10 \times 10 \text{ km}^2$  (Suguta Area) and their petrography and petrochemistry are described. A decrease in degree of silica-undersaturation with time from alkali basalts to transitional basalts can be recognized. Successive decrease in depth of segregation of primary magmas can explain the temporal variation in chemical composition.

### INTRODUCTION

The East African Rift is characterized by profuse volcanism with a total volume of ejecta of  $500,000 \text{ km}^3$  (Baker *et al.* 1972). Petrologic study of the volcanic rocks would, therefore, provide essential information about the evolution of the rift. Based on the compilation of numerous geochronological and petrochemical data (Harris, 1969; Williams, 1972; Lippard and Truckle, 1978; Baker *et al.*, 1978; Barberi *et al.*, 1982), the chemical variation of the volcanic rocks in both time and space can be roughly summarized as follows:

— a decrease in alkalinity and degree of silica-undersaturation occurs 1) with time as well as 2) across the rift towards the axis and 3) along the rift northward. However these trends are still so rough and qualitative that we cannot understand their geologic implications with respect to structural geological and geophysical data. More detailed data concerning the chemical variation are required.

The purpose of this paper is to examine the temporal variation in basalt chemistry in the rift near Samburu and to understand the evolution of the rift based on recent experimental studies on the magma genesis (e.g. Jaques and Green, 1979, 1980; Takahashi *et al.*, 1981; Takahashi and Kushiro, 1983).

New petrochemical and petrographical data concerning the volcanic rocks from the Samburu Hills, Kenya, where a sequence of Miocene, Plio-Pleistocene and Recent basalts was established during the 1982 Japan/Kenya expedition, will be described. In order to eliminate the effect of spatial variation and to determine the temporal variation in chemistry, the sites from which the samples were collected were confined to a small area of  $10 \times 10 \text{ km}^2$ . Petrologic investigations were mainly carried out on relatively magnesian basalts.

### FIELD OCCURRENCES

The investigated area is situated on the eastern flank of the Suguta Valley, 50 km to the south

of Lake Turkana and 30 km west of Baragoi. Preliminary surveys were done around Nachola Village and to the northwest of Baragoi. The former area is called Suguta Area, the latter Baragoi Area (Fig. 1). Volcanic rocks in both areas are composed mainly of basaltic lava flows intercalated with lava flows and welded tuffs of more differentiated rock, such as trachyte and alkali rhyolite. The detailed geology and stratigraphy of these areas are given by Makinouchi *et al.* (1984).

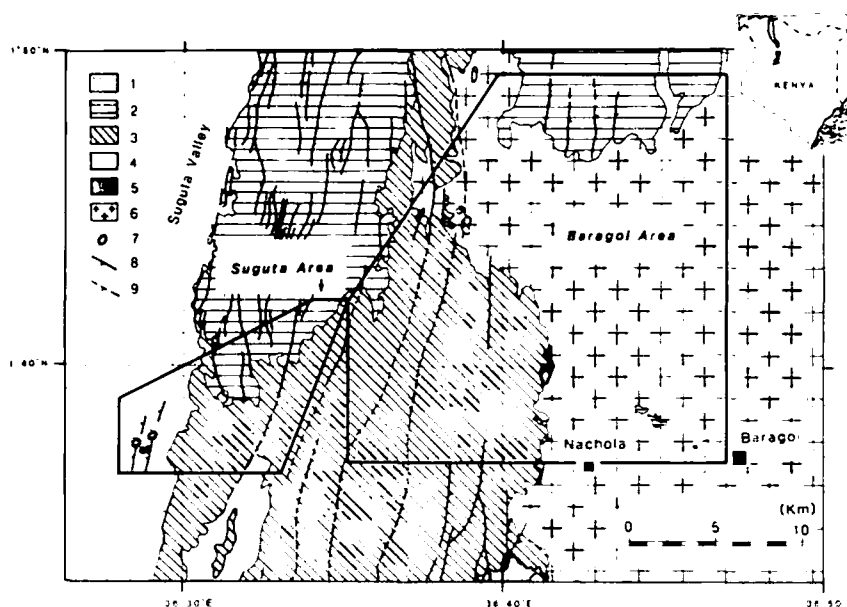


Fig. 1: Index map showing positions of the "Suguta Area" and the "Baragoi Area". Based on Baker's geological map (1963), which is simplified and slightly modified. 1; Superficial deposits. 2; Volcanic rocks of the Tirr Tirr Formation. 3; Volcanic rocks of the Nagubarat, Kongia, Aka Aiteputh and Nachola Formations. 4; Sedimentary rocks of the Namurungule Formation. 5; Sedimentary rocks of the Nachola Formation. 6; Basement rocks (Pre-Cambrian). 7; Scoria cones. 8; Faults, observed. 9; Faults, inferred.

The volcanic rocks of the Suguta Area are divided into five formations separated from each other by unconformities. From lower to upper these are the Aka Aiteputh Formation, the Namurungule Formation, the Kongia Formation, the Nagubarat Formation and the Tirr Tirr Formation.

The Aka Aiteputh Formation is mainly composed of basaltic rocks (including some ankaramites and hawaiites) which are rarely interstratified with trachytic lava flows and welded tuffs. The K-Ar age of the uppermost lava of this formation is 12 Ma (Matsuda *et al.*, 1984). The Namurungule Formation is composed of sedimentary rocks, including mud flow deposits and lake deposits. The Kongia Formation is composed of basaltic rocks. The K-Ar age of the lowermost lava of this formation is 6 Ma (Matsuda *et al.*, 1984). Strata in these three formations generally dip several tens of degrees westwards.

Alkali basalt lava flows and necks, which unconformably overlie the Aka Aiteputh, Namurungule and Kongia Formations and dip westwards at about ten degrees, belong to the Nagubarat Formation.

Nearly horizontal basalt and alkali rhyolite lava flows, which unconformably overlie the Aka Aiteputh and Kongia Formations belong to the Tirr Tirr Formation. This formation was called the "Tirr Tirr series" by Baker (1963). The K-Ar age of the alkali rhyolite of this formation is about 4 Ma (Baker *et al.*, 1971).

Besides the above five formations several scoria cones with or without lava flows form alignments along normal faults in the Sugura Valley. The scoria cones preserve their original topography very well (Plate 1, Fig. 1) and are considered to be of Recent Age.

In the Aka Aiteputh Formation samples were collected from several horizons. Stratigraphic relationships among most of the horizons are clear, although for the uppermost part of this formation two samples may have been collected from the same horizons, because two routes were used when the rocks were collected. In the Kongia Formation samples were collected from many horizons along a route where the stratigraphic relationships are clear. Samples were collected from two lava flows in the Nagubarat Formation, but the stratigraphic relationship between the two flows is not clear at present. In the Tirr Tirr Formation samples were collected from many stratigraphic horizons. Only one basalt sample was collected from a scoria cone in the Suguta Valley. Thus volcanic rocks of various ages, from Miocene to Recent, were collected from the Suguta Area.

In the Baragoi Area occur the Nachola Formation and younger unnamed basaltic lava flows of unknown sequence. The Nachola Formation consists of alternations of volcanic rocks and sedimentary deposits. Strata of this formation dip several tens of degrees westwards. This formation is presumed to correlate with or to underlie the Aka Aiteputh Formation. The younger basaltic lava flows unconformably overlie the Pre-Cambrian Basement and/or the Nachola Formation. They are nearly horizontal and may correlate to the Tirr Tirr Formation. Samples were randomly collected in this area.

In this paper volcanic activity of the Suguta Area is divided into four stages separated from each others by major clino-unconformities. Stage I corresponds to the Aka Aiteputh and Kongia Formations. This stage is subdivided into two substages corresponding to the two formations. Stage II to IV corresponds to the Nagubarat and Tirr Tirr Formations and the volcanics in the Suguta Valley, respectively.

## ANALYTICAL METHODS

Most of the whole rock analyses (10 oxides) were done with the Rigaku XRF of the University of Tokyo. Details of the analytical method were reported by Matsumoto and Urabe (1980). Chemical compositions of minerals were determined by electron probe microanalyzer model JEOL JXA-5 of the Geological Institute and JEOL JXA-733 of the Ocean Research Institute of the University of Tokyo. The analytical procedure is similar to that given by Nakamura and Kushiro (1970), and the correction procedure of Bence and Albee (1969) was followed.

## PETROGRAPHY

### (1) Basaltic rocks

#### *Description of representative samples*

Basaltic rocks occur as lava flows or sills all over the district. Only lava flows will be considered in this paper. Basaltic rocks can be divided into three types based on their petrographic features as follows;

- (i) Ankaramite (Aka Aiteputh and Kongia Formations)
- (ii) Olivine basalt (all the formations)
- (iii) Hawaiite (Aka Aiteputh, Kongia and Tiri Tiri Formations)

The six samples on which K-Ar age determinations were carried out (82101504, 82101501, 82082401, 82100106, 82100113 and 82100114) are also described below.

(i) Ankaramite

Basaltic rocks characterized by abundant olivine and clinopyroxene phenocrysts (more than 20 vol.%) are named ankaramite in this paper. Most of them have normative nepheline, but ankaramites in the Kongia Formation (e.g. 82083106) have normative hypersthene.

Table 1

Modal analyses of basaltic rocks in the Suguta Area.

Sample No.	ol	cpx	pl	mt	gm
82083101	0.6	0.2	1.1	0.0	98.1
N-32	4.0	1.6	0.0	0.0	94.4
82082501	0.6	0.1	0.6	tr	98.7
82100407	0.0	0.0	0.0	0.0	100.0
82100406	0.9	1.1	10.3	0.0	87.3
82100403	0.1	0.0	1.0	0.0	98.9
82083104	21.0	9.2	0.0	0.0	69.8
82083106	11.1	10.4	0.0	0.0	78.5
82083107	0.0	0.0	0.0	0.0	100.0
82083108	0.0	0.0	0.0	0.0	100.0
82083109	0.5	0.0	2.2	0.0	97.3
82083110	3.7	1.3	9.8	0.0	85.2
82100103	1.5	1.5	0.0	tr	97.1
82100104	0.0	0.0	0.0	0.0	100.0
82100105	0.8	0.0	1.5	0.0	97.7
82100106	0.6	0.0	0.9	0.0	98.5
82100110	3.9	7.9	0.0	0.0	88.2
82100113	3.5	2.6	0.1	0.1	93.7
82100114	1.0	2.5	21.2	0.2	75.3
82092801	0.9	tr	0.0	0.0	99.1
82092803	0.6	0.0	0.1	0.0	99.3
82092804	6.7	4.8	0.2	0.0	88.3
82092806	0.0	0.0	0.0	0.0	100.0
82092812	2.1	5.7	0.7	0.0	91.5
82092814	6.4	1.7	0.0	tr	91.9
82092817	12.3	29.3	0.0	0.0	58.4
82092818	0.8	5.1	1.4	0.1	92.6
82093001	10.5	14.5	0.0	tr	75.0
82100903	2.3	9.6	0.0	0.0	88.1

ol: olivine cpx: clinopyroxene pl: plagioclase mt: magnetite gm: groundmass

Sequence is the same as Fig. 8.

82093001 (Aka Aiteputh Formation): This rock is one of the most silica-undersaturated basaltic rocks in the Samburu District (15 wt% normative nepheline). It contains euhedral to subhedral olivine and augite phenocrysts. The total amount of phenocrysts is 25 vol.% (Table 1). These phenocrysts contain inclusions of euhedral chromian spinel. Microphenocrysts are olivine, augite and an opaque mineral. The augite microphenocrysts show conspicuous hourglass structure. Olivine is partly replaced by serpentine, especially along cleavage planes. Groundmass shows intergranular to intersertal texture. It is composed of lath-shaped plagioclase, euhedral titanite, olivine and opaque minerals with interstitial alkali feldspar, zeolite, nepheline and a green clay mineral. The clay mineral is considered to be altered glass. Zeolite also occurs filling a druse.

Table 2

Chemical compositions of phenocrystic minerals

	FELDSPAR			OLIVINE	
	1	2	3	4	5
SiO <sub>2</sub>	51.94	53.09	67.33	39.31	29.97
TiO <sub>2</sub>	0.15	0.16	0.00	0.01	0.01
Al <sub>2</sub> O <sub>3</sub>	29.12	29.12	18.20	0.00	0.01
FeO	0.61	0.54	0.79	8.83	65.92
MnO	0.00	0.00	0.03	0.47	2.95
MgO	0.17	0.13	0.00	49.87	0.09
CaO	13.11	12.54	0.01	0.15	0.37
Na <sub>2</sub> O	4.01	4.38	7.55	0.00	0.00
K <sub>2</sub> O	0.23	0.26	6.20	0.00	0.00
NiO	0.00	0.00	0.01	0.19	0.00
Cr <sub>2</sub> O <sub>3</sub>	0.01	0.01	0.03	0.05	0.00
V <sub>2</sub> O <sub>3</sub>	0.00	0.01	0.00	0.00	0.01
total	99.35	100.23	100.13	99.28	99.35
	O = 8	O = 8	O = 8	O = 4	O = 4
Si	2.382	2.408	3.012	0.981	1.014
Ti	0.005	0.005	0.000	0.000	0.001
Al	1.574	1.556	0.960	0.000	0.000
Fe	0.023	0.020	0.030	0.182	1.866
Mn	0.000	0.000	0.001	0.010	0.084
Mg	0.011	0.009	0.000	1.837	0.005
Ca	0.644	0.609	0.000	0.004	0.014
Na	0.356	0.385	0.655	0.000	0.000
K	0.014	0.015	0.354	0.000	0.000
Ni	0.000	0.000	0.000	0.004	0.000
Cr	0.000	0.000	0.001	0.001	0.000
V	0.000	0.000	0.000	0.000	0.000
total	5.011	5.009	5.012	3.019	2.985
An	63.50	60.32	0.03	Fo	0.25
Ab	35.14	38.18	64.90		
Or	1.36	1.50	35.07		

1: core of plagioclase microphenocryst in 82083101 (olivine basalt)

2: rim of "1"

3: core of sanidine phenocryst in 82100404 (alkali rhyolite)

4: core of olivine phenocryst in N-32 (olivine basalt)

5: core of olivine phenocryst in 82100404 (alkali rhyolite)

Table 2 (continue)

	CLINOPYROXENE						
	6	7	8	9	10	11	12
SiO <sub>2</sub>	50.52	50.37	48.72	45.31	44.11	51.68	44.77
TiO <sub>2</sub>	0.69	1.17	2.04	4.22	5.85	0.51	2.84
Al <sub>2</sub> O <sub>3</sub>	0.63	3.87	4.71	6.43	5.77	3.93	9.42
FeO	20.70	4.77	6.64	10.14	12.96	3.63	7.05
MnO	1.03	0.12	0.20	0.21	0.25	0.11	0.11
MgO	5.18	15.27	14.46	11.38	8.94	16.16	11.99
CaO	18.07	22.33	21.77	20.68	19.59	22.10	22.73
Na <sub>2</sub> O	2.36	0.32	0.65	0.51	0.78	0.42	0.43
K <sub>2</sub> O	0.03	0.00	0.00	0.01	0.00	0.01	0.01
NiO	0.04	0.05	0.06	0.00	0.00	0.00	0.00
Cr <sub>2</sub> O <sub>3</sub>	0.00	0.80	0.08	0.11	0.00	1.35	0.31
V <sub>2</sub> O <sub>3</sub>	0.00	0.03	0.01	0.13	0.04	0.00	0.00
total	99.25	99.10	99.33	99.15	98.29	99.91	99.67
	O = 6	O = 6	O = 6	O = 6	O = 6	O = 6	O = 6
Si	2.010	1.872	1.825	1.733	1.725	1.891	1.685
Ti	0.021	0.033	0.057	0.121	0.172	0.014	0.080
Al	0.030	0.170	0.208	0.290	0.266	0.170	0.418
Fe	0.689	0.148	0.208	0.324	0.424	0.111	0.222
Mn	0.035	0.004	0.006	0.007	0.008	0.003	0.004
Mg	0.308	0.846	0.807	0.649	0.521	0.881	0.672
Ca	0.770	0.889	0.874	0.847	0.821	0.866	0.916
Na	0.182	0.023	0.047	0.038	0.060	0.030	0.032
K	0.001	0.000	0.000	0.001	0.000	0.000	0.001
Ni	0.001	0.002	0.002	0.000	0.000	0.000	0.000
Cr	0.000	0.023	0.002	0.004	0.000	0.039	0.009
V	0.000	0.001	0.000	0.004	0.001	0.000	0.000
total	4.084	4.010	4.037	4.018	3.998	4.006	4.038
Wo	43.60	47.20	46.25	46.55	46.48	46.61	50.61
En	17.41	44.92	42.74	35.64	29.50	47.41	37.14
Fs	38.99	7.88	11.01	17.82	24.01	5.98	12.25
Mg/Mg+Fe	0.309	0.851	0.795	0.667	0.551	0.888	0.752

6: core of aegirine augite microphenocryst in 82100901 (sodalite trachyte)

7: core of clinopyroxene phenocryst in N-32 (olivine basalt)

8: rim of "7"

9: core of clinopyroxene microphenocryst in 82083101 (olivine basalt)

10: rim of "9"

11: core of clinopyroxene phenocryst in 82093001 (ankaramite)

12: rim of "11"

82092817 (Aka Aiteputh Formation): This rock is characterized by very abundant olivine and augite phenocrysts (about 40 vol.%) and by magnesian character of its bulk chemistry (16% MgO, FeO\*/MgO less than 0.6). Olivine is partly replaced by serpentine. Groundmass shows intersertal texture. It is composed of euhedral to subhedral plagioclase, titanaugite, olivine and an opaque mineral with interstitial zeolite, alkali feldspar and a green clay mineral. A small amount of secondary carbonate mineral occurs in the groundmass.

**Table 3**  
Representative bulk chemical data determined by XRF

Sample No.	SiO <sub>2</sub>	TiO <sub>2</sub>	Al <sub>2</sub> O <sub>3</sub>	FeO*	MnO	MgO	CaO	Na <sub>2</sub> O	K <sub>2</sub> O	P <sub>2</sub> O <sub>5</sub>
82083101	47.64	3.05	15.47	12.11	0.19	6.26	11.19	2.57	0.97	0.55
82100407	49.55	3.19	13.68	14.23	0.21	4.79	10.10	2.92	1.04	0.28
82100406	50.54	2.29	17.13	11.01	0.20	3.84	10.00	3.35	1.29	0.36
82100404	70.19	0.58	11.91	8.28	0.28	0.02	0.67	3.79	4.30	0.00
82100403	48.51	3.06	14.90	13.84	0.20	5.60	9.60	2.96	1.05	0.27
N-32	47.77	2.13	13.37	9.92	0.15	12.25	10.67	1.86	1.50	0.38
82082501	48.46	2.39	17.44	10.67	0.17	5.86	9.69	3.25	1.66	0.41
82083104	47.51	1.55	10.02	11.60	0.17	16.14	10.88	1.54	0.42	0.15
82083106	47.66	1.43	9.13	11.47	0.17	16.83	11.52	1.34	0.35	0.10
82083107	48.52	2.71	18.32	11.15	0.17	4.78	9.14	2.88	1.85	0.49
82083108	49.00	2.73	17.61	11.09	0.17	4.93	9.07	3.07	1.82	0.52
82083109	48.56	2.41	17.62	10.68	0.17	6.01	9.40	3.20	1.55	0.41
82083110	47.85	2.56	16.07	11.91	0.17	6.70	10.56	2.80	1.13	0.26
82083111**	56.28	1.59	16.97	9.28	0.22	1.86	5.20	4.85	3.31	0.42
82100103	47.83	2.33	17.40	11.13	0.17	5.70	10.79	3.39	1.04	0.22
82100104	48.97	2.72	17.65	11.04	0.18	5.15	8.49	3.54	1.80	0.48
82100105	48.10	2.37	17.23	10.58	0.17	5.79	9.39	4.34	1.66	0.39
82100110	44.79	2.61	14.47	13.34	0.24	6.99	13.07	3.26	1.03	0.22
82092801	47.83	2.27	17.28	11.27	0.18	6.26	10.15	3.10	1.35	0.31
82092803	48.13	2.29	18.00	11.02	0.17	5.10	10.35	3.13	1.47	0.34
82092804	46.11	2.03	13.46	10.86	0.18	11.94	11.85	2.81	0.49	0.27
82092806	47.93	2.32	18.30	10.32	0.19	5.85	10.70	2.69	1.37	0.34
82092812	46.59	2.05	15.45	11.32	0.18	7.12	12.92	2.93	1.14	0.29
82092814	46.57	2.25	15.58	11.03	0.19	8.42	11.49	3.26	0.84	0.37
82092817	46.04	1.46	10.00	9.38	0.15	16.03	14.15	2.20	0.51	0.09
82092818	46.36	2.46	16.70	11.82	0.20	6.10	11.52	3.15	1.06	0.61
82093001	46.05	1.70	12.22	10.14	0.18	13.26	11.47	3.65	1.17	0.17
82100901	62.51	0.68	14.80	9.14	0.36	0.57	1.68	5.18	4.92	0.17
82100903	46.96	2.03	15.28	10.10	0.19	8.43	11.44	3.73	1.55	0.28
82101501	46.49	2.57	15.88	12.68	0.19	6.90	12.21	1.91	0.88	0.29
82101504	46.13	3.25	15.29	13.74	0.21	6.15	10.99	2.46	1.17	0.61
82101202***	47.22	1.65	16.73	10.33	0.16	7.18	13.57	2.46	0.59	0.12

\* total Fe as FeO

\*\* aphyric trachytic hawaiite

\*\*\* younger olivine-augite alkali basalt in the Baragoi Area

See text for petrography of other rocks

82083106 (Kongia Formation): This rock has normative hypersthene and deviates from a typical ankaramite in its chemistry (Table 3), but in this paper it is called ankaramite for convenience. It possesses ophytic texture with augite, olivine, plagioclase and subordinate opaque minerals and glass. The plagioclase is usually lath-shaped. The olivine and augite are usually anhedral, rarely euhedral. Augite often encloses plagioclase laths poikilitically. Large olivine and augite crystals are tentatively interpreted as phenocrysts. The total amount of phenocrysts is about 40%. Olivine is usually altered to serpentine or iddingsite. Glass is usually altered to a green clay mineral.



(ii) Olivine basalt

Most of the olivine basalts in the Samburu District have normative nepheline and a few have normative hypersthene. The hypersthene normative basalts commonly contain titanaugite and have characteristics transitional between alkali and tholeiitic basalts. Olivine basalts usually carry olivine and augite phenocrysts (0 to 20 vol.%), but rarely also have significant amounts of plagioclase phenocrysts. Some lava flows of this rock type contain ultrabasic nodules.

82101504\* (Nachola Formation): This rock carries no phenocrysts other than small amounts of plagioclase microphenocrysts. Its groundmass shows an intergranular texture. It is composed of lath-shaped plagioclase, euhedral to subhedral olivine, titanaugite and an opaque mineral and a subordinate amount of apatite and interstitial alkali feldspar. A small amount of clay minerals, which may be altered glass, occurs in the interstices. Olivine is partly replaced by iddingsite.

82101501\* (Nachola Formation): This rock carries small amounts of olivine, plagioclase and augite microphenocrysts, which often possess glomeroporphyritic texture. In such cases olivine and augite are usually anhedral. Olivine is partly altered to iddingsite, while other minerals are quite fresh. Groundmass shows an intergranular texture. It is composed of lath-shaped plagioclase, euhedral olivine, titanaugite and a subhedral opaque mineral and interstitial alkali feldspar and zeolite. Glass is rarely observed in the interstices. Zeolite in a druse also occurs in this sample.

82100114\* (Aka Aiteputh Formation): This lava is characterized by abundant euhedral plagioclase phenocrysts. It also carries subhedral augite, magnetite and olivine phenocrysts. The augite shows conspicuous pleochroism from pinkish brown to pale green. Augite and plagioclase are sometimes deeply embayed. Olivine is usually replaced by iddingsite. Groundmass shows intersertal to intergranular texture. It is composed of lath-shaped plagioclase, euhedral olivine, titanaugite, an opaque mineral and subordinate amounts of apatite, and interstitial alkali feldspar, zeolite and glass. The glass is usually altered to a green clay mineral. Apatite also occurs as inclusions in plagioclase, augite or olivine phenocrysts.

82100113\* (Aka Aiteputh Formation): This rock contains euhedral to subhedral augite, olivine and small amounts of plagioclase phenocrysts. The olivine is partly altered to iddingsite. The augite shows pleochroism from pinkish brown to pale green and is sometimes rounded. Magnetite inclusions are sometimes found in olivine and augite phenocrysts. Groundmass possesses an intergranular texture. It is composed of lath-shaped plagioclase and euhedral titanaugite, olivine and an opaque mineral, and interstitial alkali feldspar. Brown glass is rarely observed in the interstices.

N-32 (Nagubarat Formation): This rock is the most magnesian rock in the district with the exception of ankaramites. Phenocrysts are composed of euhedral to subhedral olivine and augite. Euhedral chromian spinel and magnetite occur enclosed by olivine and/or augite phenocrysts. Olivine sometimes encloses dendritic magnetite. Groundmass, which shows intersertal texture, is composed of lath-shaped plagioclase and anorthoclase, euhedral olivine, titanaugite, an opaque mineral and subordinate apatite, and interstitial alkali feldspar, analcite, glass and cossyrite. Two types of glass (brown and colorless) are observed. Small spheres of brown glass (about 1  $\mu\text{m}$  in diameter) occur enclosed in colorless glass, indicating liquid immiscibility at the later stage of solidification of a magma (Philpotts, 1979; Fujii *et al.*, 1980). Analcite syenite ocelli (Philpotts,

---

\*Samples used for K-Ar age determinations.

1978), up to several mm in diameter are observed in some slices of this rock.

This rock sometimes carries fragments of ultrabasic rock (mainly dunite and wehrlite) and felsic plutonic rock made of mainly quartz and sodic plagioclase. The felsic fragments are presumed to have originated from the Pre-Cambrian Basement. The quartz and sodic plagioclase crystals are corroded and enclosed by fine-grained clinopyroxene jackets.

82083101 (A scoria cone in the Suguta Valley): This rock contains small amounts of olivine, titanaugite and plagioclase microphenocrysts (2 vol.% as a whole). These minerals sometimes show glomeroporphyritic textures. Plagioclase microphenocrysts contain inclusions of euhedral olivine, titanaugite or an opaque mineral. Porous groundmass shows intersertal to intergranular texture. It is composed of lath-shaped or acicular plagioclase, acicular titanaugite, euhedral olivine, an opaque mineral and subordinate apatite and interstitial alkali feldspar and brown glass.

### (iii) Hawaiite

Basaltic rocks with relatively leucocratic groundmass are here named hawaiite. Plagioclase is often a dominant phase of phenocryst in this type of rock.

82100106\* (Kongia Formation): This rock is aphyric, carrying small amounts of plagioclase and olivine microphenocrysts (less than 1 vol.%). Some plagioclase microphenocrysts contain abundant glass inclusions. Groundmass possesses an intergranular texture. It is composed of lath-shaped plagioclase and euhedral olivine, titanaugite, an opaque mineral and subordinate apatite, and interstitial glass and alkali feldspar. Olivine is sometimes replaced by iddingsite or a clay mineral. Secondary chalcedony often fills druses or replaces the interstitial glass.

82082401\* (Kongia Formation): This rock is nearly aphyric. There are aggregates of a fine opaque mineral, clinopyroxene and feldspar up to 0.1 mm in diameter, which may be break-down products of hornblende. Groundmass shows an intergranular to intersertal texture. It is composed of lath-shaped plagioclase, and euhedral titanaugite, olivine, an opaque mineral and apatite, euhedral to subhedral cossyrite and hornblende, and interstitial alkali feldspar and analcite. Olivine is usually altered to iddingsite. Small amounts of a green clay mineral, which is presumed to be altered glass, occur in the interstices. Small amounts of secondary carbonate mineral occur in the groundmass.

82083113 (Kongia Formation): This rock contains abundant plagioclase (about 30 vol.%) and small amounts of olivine and titanaugite phenocrysts. The olivine is usually replaced by a carbonate mineral. Plagioclase crystals are up to 1 cm in length and contain the inclusions of glass, titanaugite, olivine or opaque minerals. Groundmass shows a subophytic texture. It is composed of lath-shaped plagioclase and anorthoclase, and euhedral or anhedral titanaugite, olivine, opaque minerals and apatite, and anhedral alkali feldspar, analcite and a secondary green clay mineral. Alkali feldspar sometimes occurs fringing plagioclase.

### *Phenocryst assemblages and modal abundances*

Basaltic rocks including ankaramite and hawaiite contain 0% to 40% phenocrysts of olivine, clinopyroxene and plagioclase. Magnetite microphenocrysts occur sparsely in some samples. In magnesian basaltic rocks of the Suguta Area (here defined by  $\text{FeO}^*/\text{MgO}$  less than 3.0 in bulk composition), the total volume percent of phenocrysts, modal ratio among olivine, clinopyroxene and plagioclase phenocrysts and  $\text{FeO}^*/\text{MgO}$  ratio of the groundmass are illustrated in Fig. 2. The chemical composition of the groundmass is estimated by subtracting chemical compositions of phenocrysts from a bulk chemical composition.

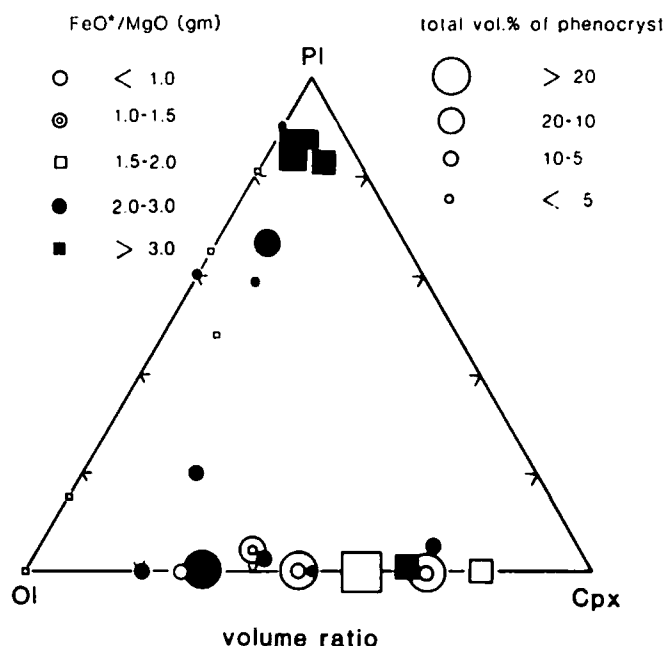


Fig. 2: Modal ratio among olivine (ol), clinopyroxene (cpx) and plagioclase (pl) phenocrysts of magnesian basaltic rocks. Total volume percent of phenocrysts is expressed by the size of symbols.

Phenocrysts in rocks which contain less than 5 vol.% of phenocrysts are generally small and there is size continuity between the phenocrysts and the groundmass crystals. For such samples crystals more than 0.2 mm in length are tentatively called phenocrysts. In contrast there is no size continuity between the phenocrysts and the groundmass crystals in rocks with more than 5 vol.% of phenocrysts. Phenocrysts in rocks with less than 5 vol.% of phenocrysts may have crystallized at the same time as the groundmass, while those in rocks with more than 5 vol.% of phenocrysts, on the other hand, would represent phases which crystallized in a magma chamber. Among rocks with more than 5 vol.% of phenocrysts, plagioclase is abundant only in rocks with a relatively iron rich groundmass ( $\text{FeO}^*/\text{MgO}$  ratio is more than 2.0) (Fig. 2). Rocks with a relatively magnesian groundmass ( $\text{FeO}^*/\text{MgO}$  less than 2.0) have a phenocryst assemblage consisting of olivine + clinopyroxene (Fig. 2). The  $\text{FeO}^*/\text{MgO}$  ratio represents the degree of fractional crystallization, because fractionation of ferro-magnesian minerals results in substantial increase of  $\text{FeO}^*/\text{MgO}$  in the residual liquid. Consequently it is inferred that the phenocryst assemblage changed from olivine + clinopyroxene to olivine + clinopyroxene + plagioclase during crystallization of the magma. Olivine may precipitate first in a primary magma after the segregation from mantle peridotite, because primary magmas should be saturated with olivine during partial melting, and because the olivine primary field expands as pressure decreases. Thus it is concluded that the crystallization sequence of the basaltic magma of the Samburu District was olivine to clinopyroxene to plagioclase.

#### *Grain size distribution of phenocrysts*

The grain size distribution of phenocrysts is here determined for those samples with more than

5 vol.% of phenocrysts. The length of each phenocryst was measured in thin sections. In general, because a thin section does not cut through the central part of the phenocryst, lengths of crystals are underestimated. We can, therefore, detect only relative differences between samples. Olivine, clinopyroxene and plagioclase phenocrysts have a similar aspect ratio (1 to 3), but most magnetite microphenocrysts have an aspect ratio of nearly 1. Phenocryst distribution within a sample is megascopically isotropic so that the modal analyses and the obtained grain size distribution are considered to be independent of the orientation of the section.

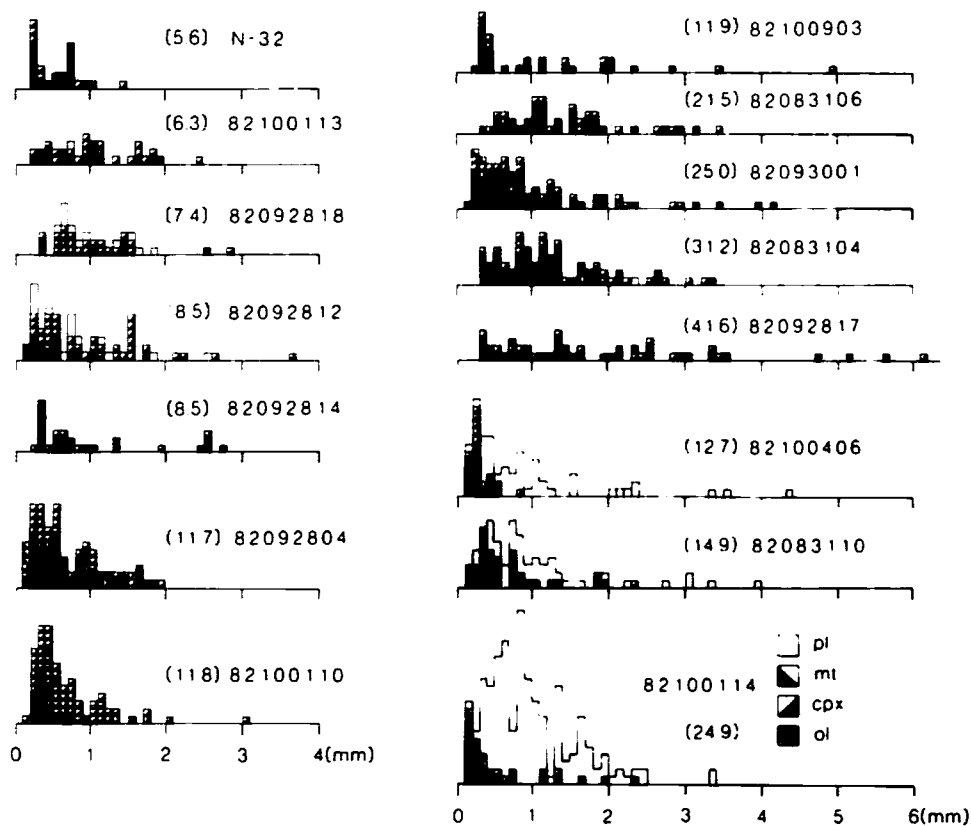


**Fig. 3:** Size distribution of phenocrysts of magnesian basaltic rocks. Numbers in parentheses indicate total volume percent of phenocrysts in each sample. pl: plagioclase. mt: magnetite. cpx: clinopyroxene. ol: olivine.

Two features can be recognized in Fig. 3. (1) Plagioclase is larger than olivine or clinopyroxene within a given sample (e.g. 82100114). (2) The samples with smaller amounts of phenocrysts are depleted in large phenocrysts in comparison with phenocryst-rich samples. Assuming that the original magma has the same initial size distribution of phenocrysts, subsequent magmas with smaller amounts of phenocrysts would be selectively depleted in large or dense phenocrysts. This is considered to result from the fact that larger or denser phenocrysts have a greater terminal velocity, and would be selectively fractionated from the magma.

### Mineralogy

Representative analyses of phenocrystic minerals in basaltic rocks are listed in Table 2.

**Olivine:** Olivine is common especially in magnesian basalts and ankaramites. In most samples it is less than 2 mm in diameter, but in a few ankaramites it attains a size of 5 mm. Picotite inclusions are commonly found. Two kinds of zoning are recognized. Olivine in basaltic rocks is usually characterized by gentle normal zoning at the core which is surrounded by a narrow rim which is strongly zoned (Fig. 4 type-B). In ankaramites, on the other hand, olivine phenocrysts generally have a large flat core (up to 5 mm in diameter) with a normally zoned rim (Fig. 4 type-A).

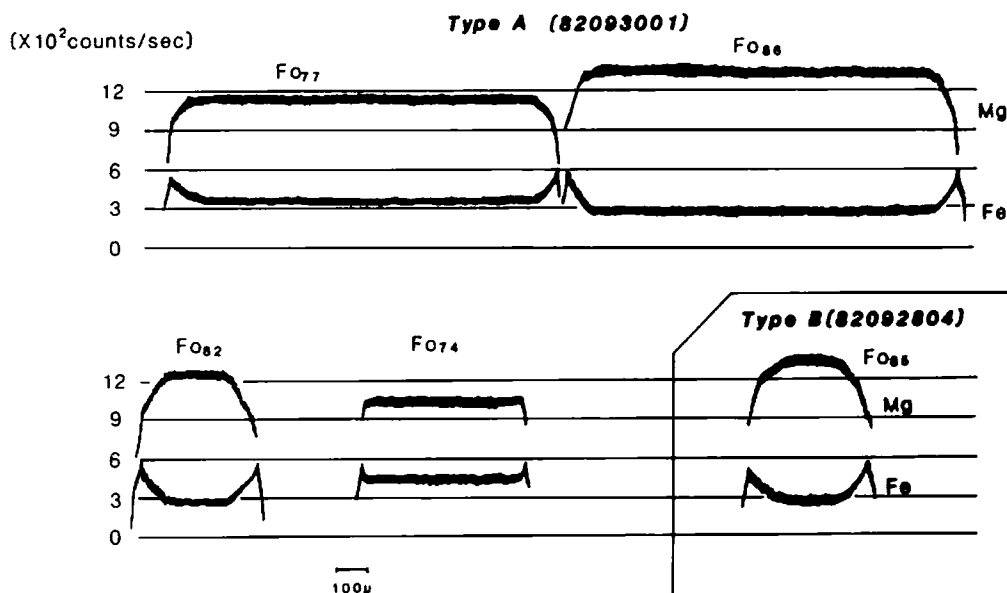


Fig. 4: Zoning profiles of olivine phenocrysts. For definitions of "type-A" and "type-B" see text.

The zoning profile of type-B olivine crystals is similar to the pattern of growth zoning which is obtained numerically (Maaløe and Hansen, 1982; Sato and Banno, 1983). That of type-A crystals, however, seems not to be explained by the growth zoning. Diffusion homogenization would have affected the profile (Koyaguchi in prep.). The forsterite content of each flat core of type-A crystals varies from crystal to crystal within a single sample.

The forsterite content of the core is roughly correlated to the bulk chemical composition, that is, the more magnesium rocks carry the more magnesian olivine phenocrysts. The ratio of  $\text{FeO/MgO}$  in olivine and  $\text{FeO/MgO}$  in bulk chemical composition (K-value) is around 0.3 in sample N-32 (Fig. 5). Roeder and Emslie (1970) proposed that Mg-Fe exchange coefficient between basaltic liquid and the coexisting olivine is about 0.3 for a wide range of temperatures and chemical compositions. The bulk chemical composition of N-32, therefore, probably represents the chemical composition of the liquid in which the core of the olivine phenocrysts was crystallized.

**Clinopyroxene (augite):** Clinopyroxene is similar or larger in size than olivine phenocrysts and is

sometimes up to 2 cm long in ankaramites. Clinopyroxene has a generally flat or mildly normally zoned core with the rim showing conspicuous normal zoning. The Mg/Mg+Fe ratio of the core is generally similar to that of coexisting olivine phenocrysts. Hourglass structure is common especially in microphenocrystic clinopyroxene.

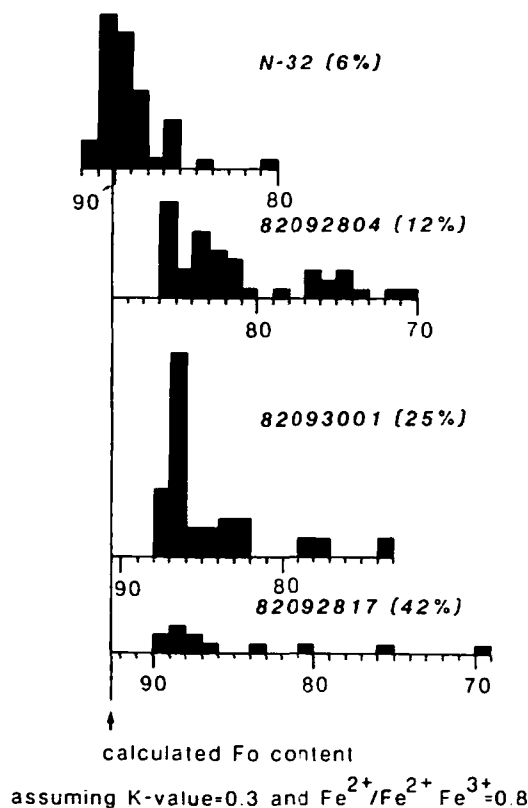


Fig. 5: Frequency diagram of forsterite content of core of olivine phenocrysts. Total volume percent of each sample is also shown.

The  $\text{Al}_2\text{O}_3$  and  $\text{TiO}_2$  content increases with decrease of the Mg/Mg+Fe ratio, namely from core to rim except in sample 82083101 where the  $\text{Al}_2\text{O}_3$  content decreases from core to rim (Fig. 6). The rate of enrichment of either the  $\text{Al}_2\text{O}_3$  or the  $\text{TiO}_2$  content against decreasing Mg/Mg+Fe is not variable among the analyzed samples and is independent of the degree of silica-undersaturation of the host rocks, i.e. normative nepheline content (Fig. 6).

**Plagioclase:** Plagioclase phenocrysts are common especially in hawaiite. Plagioclase possesses flat or mildly normal zoning. The anorthite content of the core varies from sample to sample from  $\text{An}_{70}$  to  $\text{An}_{50}$ .

## (2) Differentiated Rocks

Differentiated rocks from the Samburu District are divided into four types based on their petrographic features and mode of emplacement.

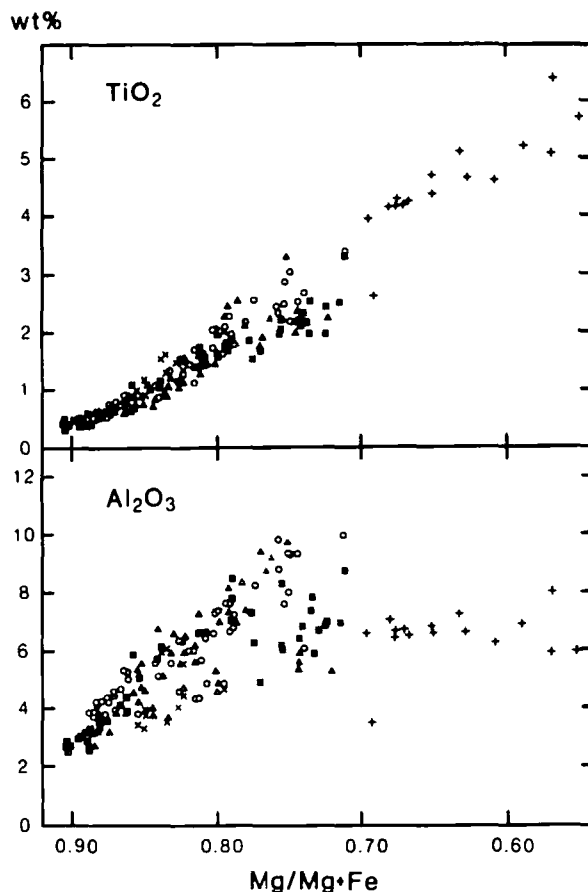


Fig. 6:  $\text{Al}_2\text{O}_3$  and  $\text{TiO}_2$  content against  $\text{Mg}/\text{Mg}+\text{Fe}$  mole ratio of clinopyroxene phenocrysts of basaltic rocks with variable normative nepheline contents (wt% ne.) Symbol +: 82083101 (0 wt% ne). Symbol x; N-32 (0.23 wt% ne). Open circle; 82092804 (6.78 wt% ne). Solid square; 82092817 (9.90 wt% ne). Open triangle; 82093001 (15.6 wt% ne).

- (i) Phonolitic trachyte lava flow (Nachola Formation)
- (ii) Sodalite trachyte lava flow (Aka Aiteputh Formation)
- (iii) Trachyte welded tuff (Nachola and Aka Aiteputh Formations)
- (iv) Alkali rhyolite lava flow (Tirr Tirr Formation)

(i) Phonolitic trachyte lava flow

Phonolitic trachyte lava flows occur about 1 km west of Nachola Village and form flat topographic features. They contain anorthoclase, ferroaugite, olivine, magnetite and apatite phenocrysts. Anorthoclase occurs as long prismatic crystals, up to 1 cm in length. It is characterized by conspicuous twinning. Ferroaugite and olivine are euhedral and up to 0.2 mm in length. Olivine is commonly replaced by a carbonate mineral. Magnetite and apatite are euhedral and up to 0.1 mm in size. Ferroaugite, magnetite and apatite are often enclosed by a large anorthoclase phenocryst.

Groundmass usually possesses intersertal texture and is composed of lath-shaped or acicular anorthoclase and euhedral clinopyroxene, magnetite and apatite and interstitial brown and colorless glass, cossyrite, and zeolite. Acicular anorthoclase enclosing fine-grained opaque minerals and glass often forms spherulites up to several mm in diameter. This rock corresponds to the phonolite lava flow depicted in Baker's geological map (1963). It is here considered to be a variety of trachyte, because of the scarcity of modal nepheline and its relatively low alkalinity.

(ii) Sodalite trachyte lava flow

Several lava flows of sodalite trachyte occur in the eastern part of the Suguta Area. They contain no phenocrysts but small amounts of microphenocrystic sodalite and anorthoclase are present. Some sodalite microphenocrysts have decomposed to form aggregates of fine-grained nepheline. Groundmass shows trachytic texture and is composed of lath-shaped anorthoclase, anhedral aegirine augite and small amounts of glass, opaque minerals, sodalite and zeolite.

(iii) Trachyte welded tuff

A red trachyte welded tuff about 20 m thick occurs in the eastern part of the Suguta Area. It contains sanidine phenocrysts and essential fragments. The essential fragments, which are up to several tens of cm in size, contain prismatic sanidine phenocrysts several mm in length. Most of the fragments are glassy, but some are crystalline and possess a trachytic texture. The groundmass of the fragments is composed of lath-shaped alkali feldspar, euhedral to anhedral aegirine augite, cossyrite and apatite. Matrix is composed of glass and sanidine fragments. Eutaxitic texture is common, especially in densely welded parts. Thin gray layers of trachyte welded tuff often occur in the Nachola Formation and in the upper part of the Aka Aiteputh Formation.

Table 4

Wet chemical analyses for selective samples

	82092502	82100114	82100113	82100106	82100101	82082401
SiO <sub>2</sub>	55.47	49.03	43.95	46.76	49.70	49.23
TiO <sub>2</sub>	1.37	2.37	2.42	2.43	2.63	3.07
Al <sub>2</sub> O <sub>3</sub>	15.36	18.38	15.63	17.16	15.83	15.60
Fe <sub>2</sub> O <sub>3</sub>	2.92	3.26	4.28	3.72	5.17	3.83
FeO	4.70	5.84	8.23	7.09	5.63	7.74
MnO	0.25	0.17	0.20	0.18	0.18	0.21
MgO	1.10	3.21	7.23	5.27	3.02	3.61
CaO	3.06	9.14	12.23	8.74	6.67	6.95
Na <sub>2</sub> O	4.93	4.31	2.71	4.18	4.83	5.13
K <sub>2</sub> O	4.98	1.25	0.78	1.35	2.45	1.85
P <sub>2</sub> O <sub>5</sub>	0.33	0.87	0.49	0.54	1.02	0.55
H <sub>2</sub> O (-)	1.30	0.18	0.10	0.10	0.18	0.15
H <sub>2</sub> O (+)	4.11	2.02	2.40	2.83	3.32	2.57
total	99.88	100.03	100.65	100.35	100.63	100.49

82092502; phonolitic trachyte	(Nachola Formation)	analyzed by H. Haramura
82100114; alkali basalt	(Aka Aiteputh Formation)	
82100113; alkali basalt	(Aka Aiteputh Formation)	
82100106; hawaiite	(Kongia Formation)	
82100101; hawaiite	(Kongia Formation)	
82082401; hawaiite	(Kongia Formation)	



## (iv) Alkali rhyolite lava flow

An alkali rhyolite lava flow up to 20-30 m in thickness occurs in the Tirr Tirr Plateau north of the Samburu Hills. It possesses a porphyritic texture with prismatic sanidine and small amounts of euhedral fayalite and aegirine augite phenocrysts. These phenocrysts are up to 5 mm long. Ground-mass is usually glassy and rarely crystalline with a trachytic texture. It contains sanidine, opaque minerals, clinopyroxene and an unidentified fine-grained mineral which is thought to be devitrified glass. This rock was called trachyte by Baker (1963), but is here considered to be an alkali rhyolite because of its high silica content (about 70%).

Selective chemical compositions of these differentiated rocks are listed in Tables 3 and 4. Some chemical compositions of the constituent minerals are listed in Table 2.

## BULK CHEMISTRY

Representative major element data listed in Table 3 were analyzed by XRF and were recalculated to give a total of 100%. Wet chemical analyses of selective samples are listed in Table 4. Most of the data points fall into the region of the alkaline rock suite as defined by Macdonald and Katsura (1964) (Fig. 7).

Most of the basalts have normative nepheline assuming that  $\text{Fe}^{2+}/\text{Fe}^{2+} + \text{Fe}^{3+} = 1.0$ . Basalts

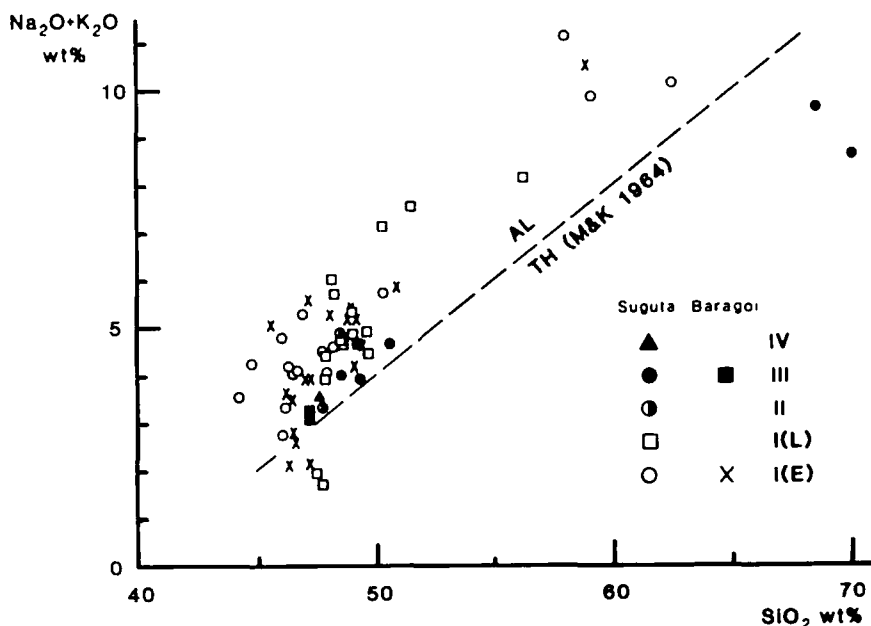


Fig. 7:  $\text{SiO}_2$  vs Alkali diagram showing relative distribution of volcanic rocks belonging to each stage in the Suguta Area. I(E); The earlier substage of Stage I. I(L); The later substage of Stage I. II; Stage II. III; Stage III. IV; Stage IV. Volcanic rocks of the Nachola Formation (X) and the younger basaltic lava flows (solid square) in the Baragoi Area are also plotted. Dashed line is the boundary between alkaline and tholeiitic rock suites as defined by Macdonald and Katsura (1964).

of the Kongia and the Tirr Tirr Formations and those in the Suguta Valley have normative hypersthene. The trachytes usually have normative hypersthene. The alkali rhyolite has normative quartz.

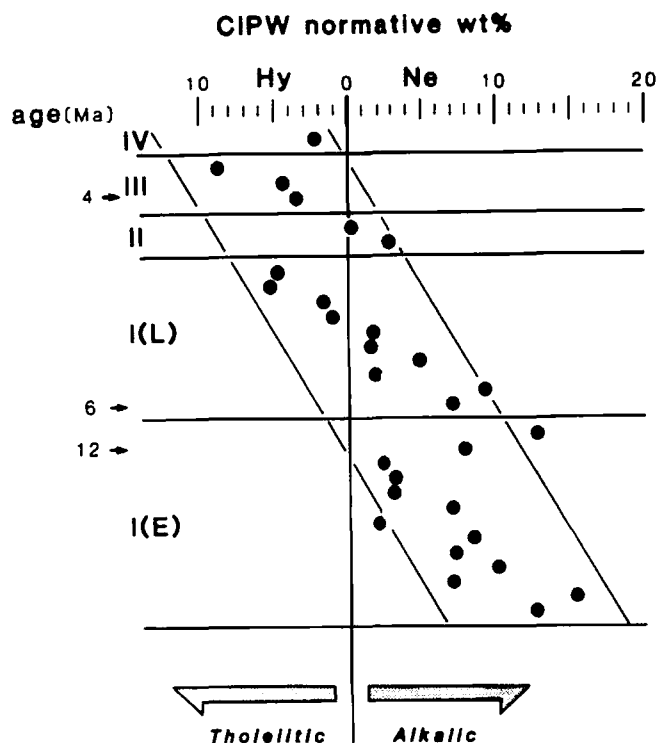


Fig. 8: Normative nepheline/hypersthene content of magnesian basaltic rocks plotted against stratigraphic sequence in the Suguta Area.

Fig. 8 shows the variation in degree of silica-undersaturation for basaltic rocks with less than 3.0 of  $\text{FeO}^*/\text{MgO}$  ratio plotted against stratigraphic sequence in the Suguta Area. The pattern which results indicates a strictly temporal variation, because the samples were obtained from a small area of  $10 \times 10 \text{ km}^2$  for which the effect of spatial variation can be considered to be negligible. A decrease in degree of silica-undersaturation with time is observed. Similar patterns have been recognized in the north Kenya and other rift systems by Lippard and Truckle (1978), Baker *et al.* (1978), and Mohr (1970).

A decrease in alkalinity in differentiated rocks ranging from trachytes (Stage I) to alkali rhyolite (Stage III) can be recognized (Fig. 7). Phonolitic trachyte and sodalite trachyte are closely associated with highly undersaturated ankaramites or basanitoids, while alkali rhyolite occurs in close association with hypersthene normative basalts. This close relation between the chemical natures of the basaltic and the differentiated rocks which erupted within a short period from a rift sector is reported from many places in the East African Rift (e.g. Barberi *et al.* 1982).

In the AFM diagram (Fig. 9) Stage III basalts show more conspicuous enrichment in  $\text{FeO}^*$  than those of Stage I, reflecting their lower alkalinity.

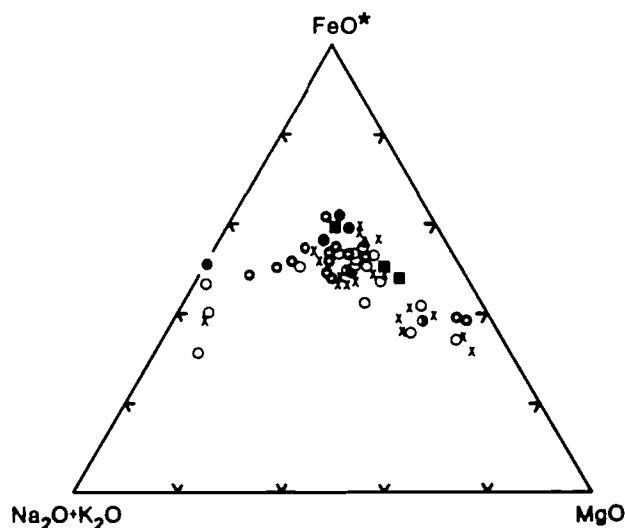


Fig. 9: Alkali-FeO\*-MgO diagram showing relative distribution of volcanic rocks of each stage. Symbols are the same as those in Fig. 7.

In Fig. 8 the vertical axis shows relative stratigraphic positions, but the spacing does not indicate any real time duration. There is a large hiatus of 6 million years between the two substages of Stage I. This hiatus in volcanism appears to be common in the northern part of the Kenya Rift judging from the data compiled by Baker *et al.* (1971). Lavas which erupted just after and just before the hiatus have a similar normative nepheline content (Fig. 8).

#### IMPLICATION OF THE TEMPORAL VARIATION IN THE CHEMISTRY OF THE BASALTIC ROCKS

The temporal variation in the chemical composition of lavas shown in Fig. 8 is considered to reflect that of primary magmas which were segregated from mantle peridotite, because the effect of fractional crystallization on the degree of silica-undersaturation of the bulk chemistry is insignificant for basaltic rocks with FeO\*/MgO less than 3.0. The effects of fractional crystallization and phenocrystic accumulation on the bulk chemistry will be discussed in detail by Koyaguchi (in prep.).

Takahashi and Kushiro (1983) proposed a normative diagram which shows the relationship between the pressure where primary magmas segregated from the upper mantle and their chemical compositions which are normatively plotted (Fig. 10). The normative nepheline content of a primary magma increases with an increase in pressure. It also increases with a decrease of the degree of partial melting.

Basaltic rocks with FeO\*/MgO less than 3.0 are plotted in Fig. 10. They are distributed across the isobaric liquid lines indicating successive decrease in depth of segregation of primary magmas from the mantle peridotite.

The depth of the segregation would depend mainly on the depth where diapiric uprise of

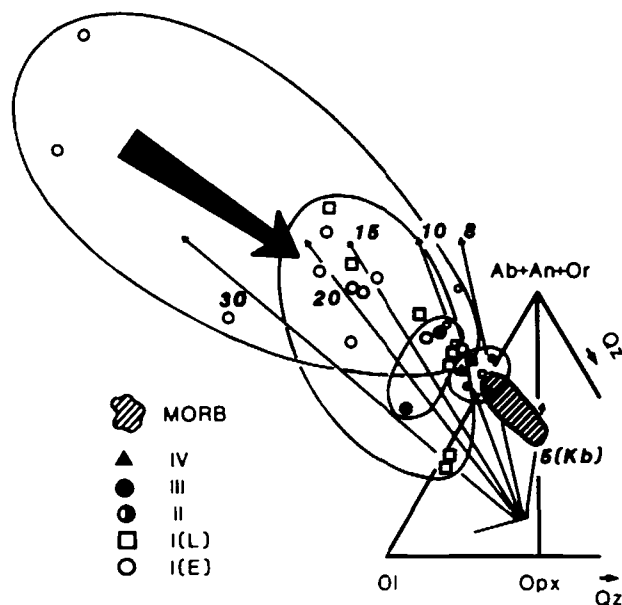


Fig. 10: Normative compositions of magnesian basaltic rocks in the Suguta Area (symbols are the same as those in Fig. 7). The isobaric compositional trend of primary magma (solid line) is from Takahashi *et al.* (1981) in ternary projection by Walker *et al.* (1979). Projected from diopside onto olivine-plagioclase-quartz plane. Large symbols: rocks with  $\text{FeO}^*/\text{MgO}$  less than 2.0. Small symbols: rocks with  $\text{FeO}^*/\text{MgO}$  between 2.0 and 3.0. Ab: albite, An: anorthite, Or: orthoclase, Qz: quartz, Ol: olivine, Opx: orthopyroxene.

mantle comes to a stop. There are at least two possible boundaries where the diapiric uprise may stop. The crust-mantle boundary is the most important boundary through which a mantle diapir is unable to move upward by buoyant force alone. The asthenosphere-lithosphere boundary would be the other important boundary where the viscosity of the mantle abruptly changes. Numerous studies on gravity and seismicity indicate that a zone of low velocity material reaches just below the crust (about 30 km in depth) beneath the East Africa Rift (Searle, 1970; Baker and Wohlenberg, 1971; Fairhead and Girdler, 1972; Fairhead, 1976; Long *et al.*, 1972; Long and Backhouse, 1976). Both boundaries, therefore, are consistent with the depth of segregation of the primary magmas of the recent basalts in the Samburu District. Maguire and Long (1976) estimated the crustal thickness away from the rift to be 46 km at most. On the other hand thickness of lithosphere away from the rift can be assumed to be around 100 km (Press, 1979; Fairhead, 1976; Knopoff and Schule, 1972). At the onset of volcanism in the rift, the boundary between the lithosphere and the asthenosphere seems to have played a role in stopping diapiric uprise, judging from the depth of segregation of magmas (about 100 km in depth). The temporal variation in the basalt chemistry can, therefore, be inferred to be related to the thinning of lithosphere (crust + lithospheric mantle).

Variation in the degree of partial melting cannot be estimated at present. Assuming the adiabatic uprise of the mantle diapir, as the diapir rises, the pressure decreases and the degree of partial melting increases. Both factors, (1) the successive decrease of pressure and (2) the successive

increase of degree of partial melting, may operate at the same time and would result in the successive decrease in degree of silica-undersaturation of the basaltic rocks of this district.

**ACKNOWLEDGEMENTS** Many thanks to Prof. H. Ishida, the chief of the expedition, of Osaka University for his invitation to the expedition and encouragement, and to Drs. T. Makinouchi of Meijo University, M. Pickford of National Museum of Kenya and T. Matsuda of Himeji Institute of Technology and Profs. S. Ishida of Kyoto University and H. Mitsushio of Kochi University for their helpful commentary during the field work. I would like to thank to Mr. Y. Nakano of Osaka University, and Mr. K. Chepboi of National Museum of Kenya who supported the field work. The first draft of the manuscript was critically read by Dr. T. Fujii of University of Tokyo. I am indebted deeply to him for his constructive criticism and improvement of the manuscript.

## REFERENCES

- Baker, B.H.. 1963. Geology of the Baragoi area. (with colored geological map) *Geol. Surv. Kenya. Rept.*, No. 53, pp. 1–74.
- Baker, B.H., R. Crossley and G.G. Goles, 1978. Tectonic and magmatic evolution of the southern part of the Kenya rift valley. In (Neumann and Ramberg eds.) *Petrology and Geochemistry of Continental Rifts*. Reidel Publ. Co., Dordrecht, Holland. 29–50.
- Baker, B.H., P.A. Mohr and L.A.J. Williams, 1972. Geology of the eastern rift system of Africa. *Geol. Soc. Am., Spec. Pap.* 136, pp. 1–67.
- Baker, B.H., L.A.J. Williams, J.A. Miller and F.J. Fitch, 1971. Geochronology of the Kenya Rift volcanics. *Tectonophys.*, 11: 191–215.
- Baker, B.H. and J. Wohlenberg, 1971. Structure and evolution of the Kenya Rift Valley. *Nature*: 229. 538–542.
- Barberi, F., R. Santacroce and J. Varet, 1982. Chemical aspects of rift magmatism. In (Palmeson ed.) *Continental and Oceanic Rifts, Geodynamics Series* vol. 8, U.S.A. pp. 223–258.
- Bence, A.E. and A.L. Albee, 1968. Empirical correction factors for the electron microanalysis of silicates and oxides. *J. Geol.*, 76: 382–403.
- Fairhead, J.D., 1976. The structure of lithosphere beneath the Eastern Rift, East Africa, deduced from gravity studies. *Tectonophys.*, 30: 269–298.
- Fairhead, J.D. and R.W. Girdler, 1972. The seismicity of the East African rift system. *Tectonophys.*, 15: 115–122.
- Fujii, T., I. Kushiro, Y. Nakamura and T. Koyaguchi, 1980. A note on silicate liquid immiscibility in Japanese volcanic rocks. *J. Geol. Soc. Japan*, 86: 409–412.
- Harris, P.G., 1969. Basalt type and African Rift Valley tectonism. *Tectonophys.*, 8: 427–436.
- Jaques, A.L. and D.H. Green, 1979. Determination of liquid compositions in experimental, high-pressure melting peridotite. *Am. Mineral.*, 64: 1312–1321.
- Jaques, A.L. and D.H. Green, 1980. Anhydrous melting of Peridotite at 0–15 kbar pressure and the genesis of tholeiitic basalt. *Contrib. Mineral. Petrol.*, 73: 287–310.
- Knopoff, L. and J.W. Schule, 1972. Rayleigh wave phase velocities for the path Addis Ababa – Nairobi. *Tectonophys.*, 15: 157–163.
- Lippard, S.J. and P.H. Truckle, 1978. Spatial and temporal variation in basalt geochemistry in

- N. Kenya rift. In (Neumann and Ramberg eds.) *Petrology and Geochemistry of Continental Rifts*, Reidal Publ. Co., Dordrecht, Holland pp. 123–131.
- Long, R.E. and R.W. Backhouse, 1976. The structure of the Western flank of the Gregory Rift. Part II. The mantle. *Geophys. J. R. astr. Soc.*, 21: 13–31.
- Long, R.E., R.W. Backhouse, P.K.H. Maguire and K. Sunder Lingham, 1972. The structure of East Africa using surface wave dispersion and Durham seismic array data. *Tectonophys.*, 15: 165–178.
- Maaløe, S. and B. Hansen, 1982. Olivine phenocrysts of Hawaiian olivine tholeiite and oceanite. *Contrib. Mineral. Petrol.*, 81: 203–211.
- Macdonald, G.A. and T. Katsura, 1964. Chemical composition of Hawaiian lavas. *Jour. Petrol.*, 5, Part I: 82–133.
- Maguire, P.K.H. and R.E. Long, 1976. The structure on the western flank of the Gregory Rift (Kenya). Part I. The crust. *Geophys. J. R. astr. Soc.*, 44: 661–688.
- Makinouchi, T., T. Koyaguchi, T. Matsuda, H. Mitsushio and S. Ishida, 1984. Geology of the Nachola Area and the Samburu Hills, West of Baragoi, Northern Kenya. *African Study Monographs, Supplementary Issue 2*: 15–44.
- Matsuda, T., M. Torii, T. Koyaguchi, T. Makinouchi, H. Mitsushio and S. Ishida, 1984. Fission-track, K-Ar Ages Determinations and Palaeomagnetic Measurements of Miocene Volcanic Rocks in the Western Area of Baragoi, Northern Kenya: Ages of Hominoids. *African Study Monographs, Supplementary Issue 2*: 57–66.
- Matsumoto, R. and T. Urabe, 1980. An automatic analysis of major elements in silicate rocks with X-ray fluorescence spectrometer using fused disc samples. *J. Japan. Assoc. Miner. Petrol. Econ. Geol.*, 75: 272–278. (in Japanese).
- Mohr, P.A., 1971. Ethiopia rift and plateaus: Some volcanic petrochemical differences. *J. Geophys. Res.*, 76. 1967–1984.
- Nakamura, Y. and I. Kushiro, 1970. Compositional relations of coexisting orthopyroxenes, pigeonite and augite in a tholeiitic andesite from Hakone volcano. *Contrib. Mineral. Petrol.*, 26: 265–275.
- Philpotts, A.R., 1978. Rift-associated igneous activity in Eastern North America. In (Neumann and Ramberg eds.) *Petrology and Geochemistry of Continental Rifts*, Reidel Publ. Co., Dordrecht, Holland pp. 135–154.
- Philpotts, A.R., 1979. Silicate liquid immiscibility in tholeiitic basalts. *J. Petrol.*, 20: Part I, 99–118.
- Press, F., 1970. Recognized earth models. *J. Geophys. Res.*, 75: 6575–6581.
- Roeder, P.L. and R.F. Emslie, 1970. Olivine-liquid equilibrium. *Contrib. Mineral. Petrol.*, 29: 275–289.
- Sato, H. and S. Banno, 1983. NiO-Fo relation of magnesian olivine phenocryst in high-magnesian andesite and associated basalt-andesite-sanukite from Northeast Shikoku, Japan. *Bull. Volcanol. Soc. Japan, Ser. 2*, 28: 141–156.
- Searle, R.C., 1970. Evidence from gravity anomalies for thinning of the lithosphere beneath the Rift Valley in Kenya. *Geophys. J. R. astr. Soc.*, 21: 13–31.
- Takahashi, E. and I. Kushiro, 1983. Melting of dry peridotite at high pressure and basalt magma genesis. *Amer. Mineral.*, 68: 859–879.
- Takahashi, E., I. Kushiro and Y. Tatsumi, 1981. Melting of a peridotite at high pressures and its

- bearing on island arc magmas. In: *Abstract 1981 IAVCEI Symposium, Tokyo*. Volcanol. Soc. Japan, Tokyo 365–366.
- Walker, D., T. Shibata and S.E. DeLong, 1979. Abyssal tholeiites from the Oceanographer fracture zone. II. Phase equilibria and mixing. *Contrib. Mineral. Petrol.*, 70: 111–125.
- Willams, L.A.J., 1972. The Kenya rift volcanism: a note on volumes and chemical composition. In (Girdler ed.) *East African Rift, Tectonophys.*, 15(1/2): 83–96.

## Explanation of Plate 1

**Fig. 1** The scoria cone in the Suguta Valley.

**Fig. 2** Ankaramite of the Aka Aiteputh Formation (82092817).

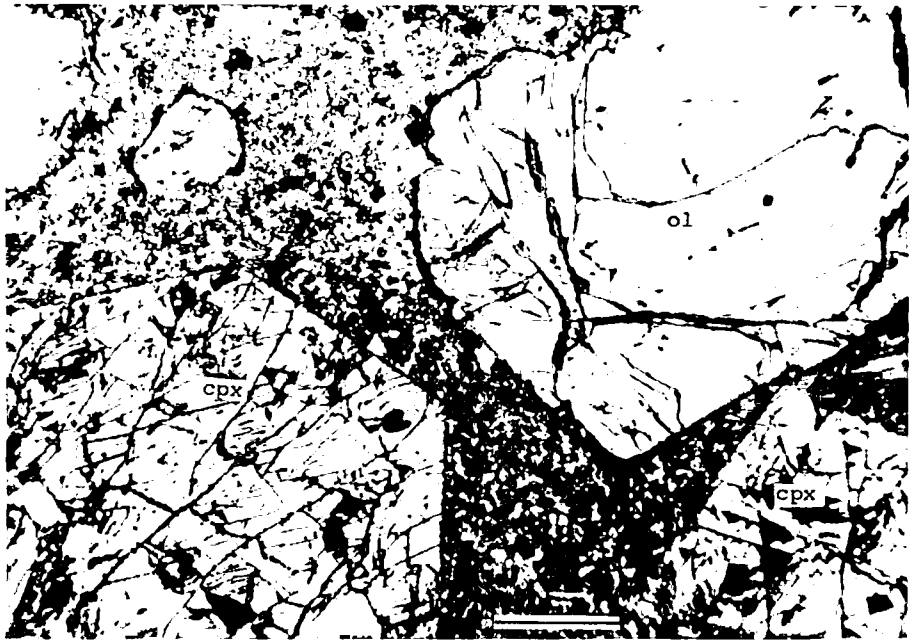
Scale bar is 0.5 mm here and after.

ol: olivine    cpx: clinopyroxene





1



2

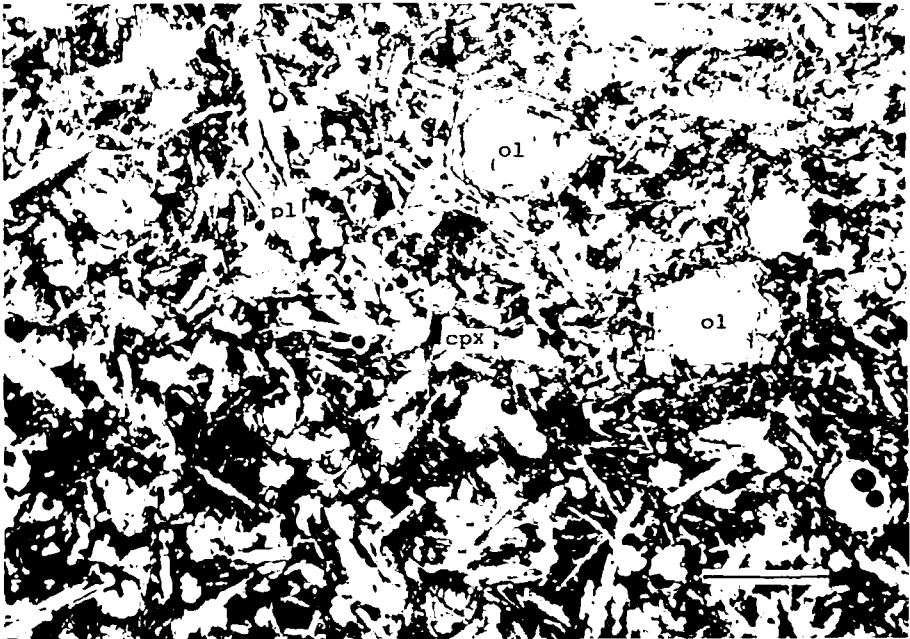
## Explanation of Plate 2

**Fig. 1** Alkali basalt of the scoria cone in the Suguta Valley (82083101).

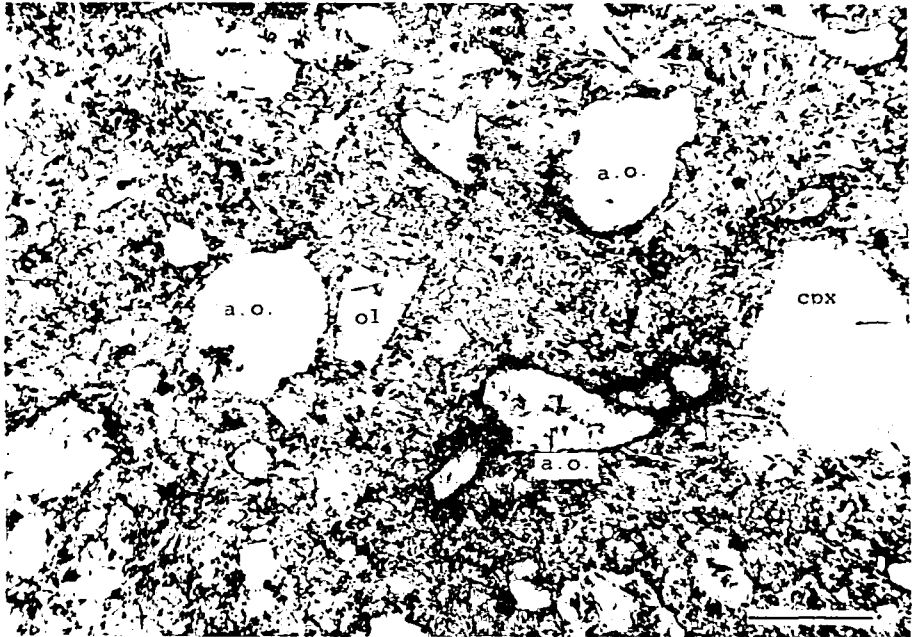
pl: plagioclase    ol: olivine    cpx: clinopyroxene

**Fig. 2** Analcite syenite ocelli in alkali basalt of the Nagubarat Formation (N-32).

a.o.: analcite syenite ocellus    ol: olivine    cpx: clinopyroxene



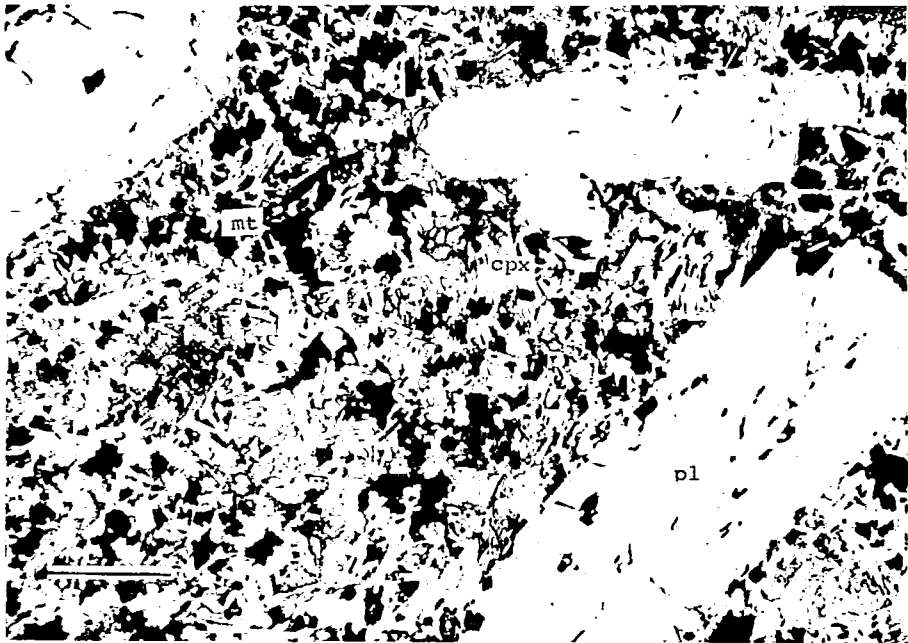
1



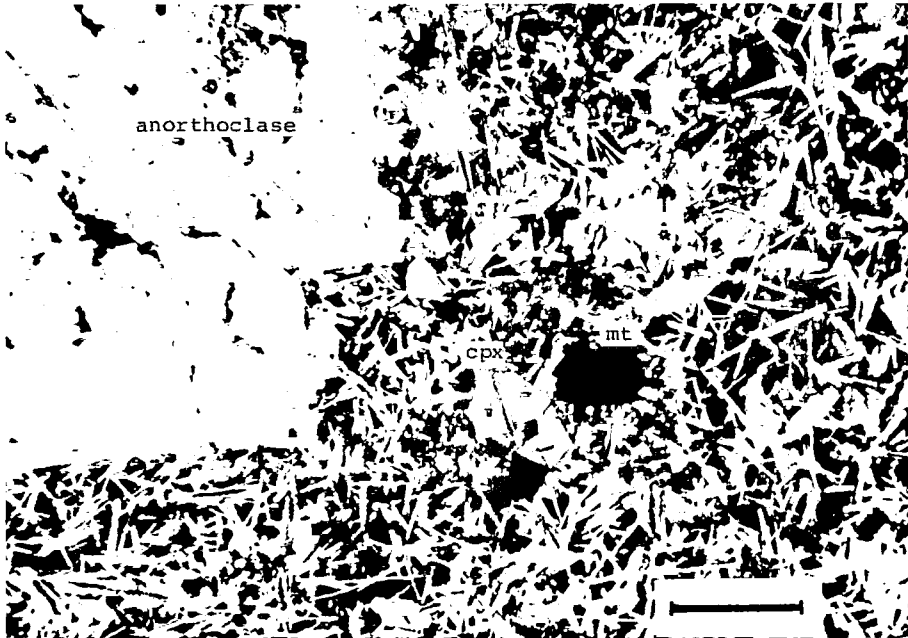
2

## Explanation of Plate 3

- Fig. 1** Hawaiite of the Kongia Formation (82083113).  
mt: magnetite cpx: clinopyroxene pl: plagioclase
- Fig. 2** Phonolitic trachyte of the Nachola Formation (82092505).  
mt: magnetite cpx: clinopyroxene



1



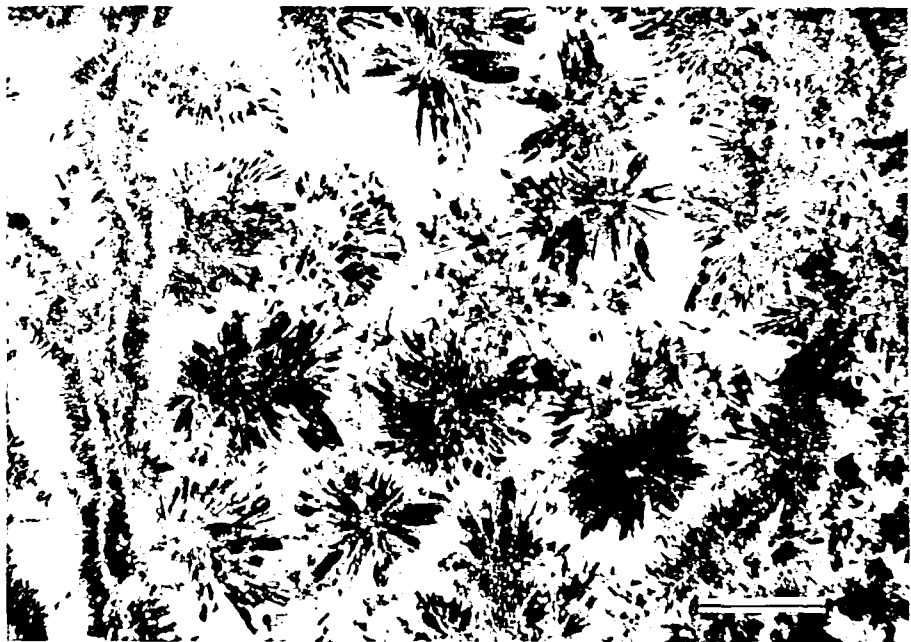
2

Explanation of Plate 4

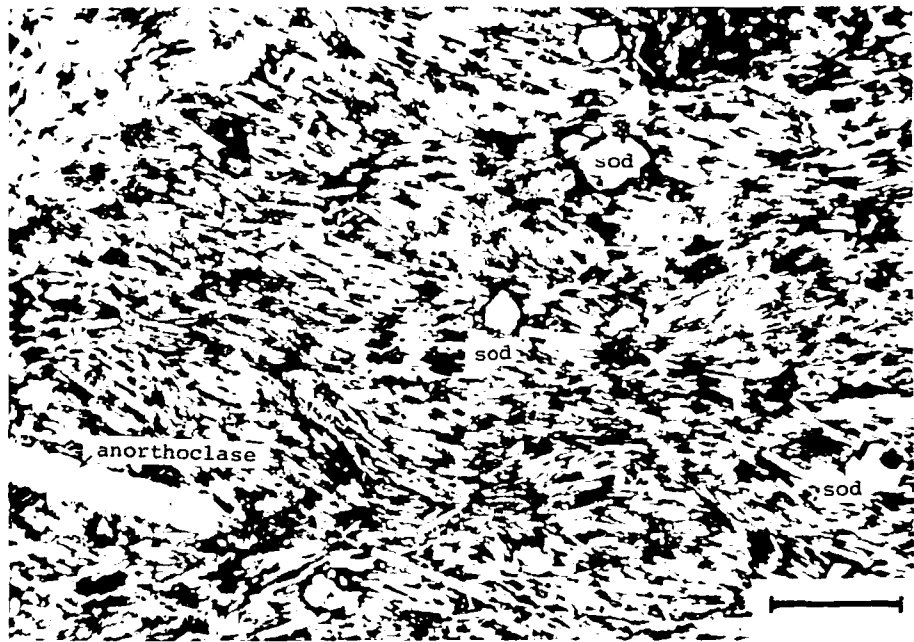
**Fig. 1** Spherulites in phonolitic trachyte of the Nachola Formation (82092503).

**Fig. 2** Sodalite trachyte of the Aka Aiteputh Formation (82100901).

sod: sodalite



1



2

## Explanation of Plate 5

**Fig. 1** Alkali rhyolite of the Turr Turr Formation (82100404).  
ol: olivine



